Instrument Science Report WFC3 1999-01

WFC3 Near-IR Channel: PSF and Plate Scale Study

Massimo Stiavelli, Christopher Hanley, Massimo Robberto
1-June-1999

ABSTRACT:

This report focuses on the PSF properties and plate scale optimization for the Near-IR channel of WFC3. We discuss how various effects lead to the final observed PSF in NICMOS Camera 2 and suggest apodization of the cold stop as a possible way to improve contrast for the Near-IR channel of WFC3. We derive a model for the pixel response of the NICMOS arrays and use this model to produce simulated images which are then employed to evaluate the WFC3 photometric accuracy as a function of pixel scale. We find that images with a pixel size of 0.15" are shallower than those with a pixel size of 0.10" by about 0.3 mag. This can be compensated by longer exposure times still maintaing a 45 percent discovery efficiency advantage for the larger pixel size. The difference between the two pixel sizes in the presence of crowding is much smaller than the deviation of both from the ideal case of infinite resolution.

1. Introduction

The purpose of this ISR is to review the main aspects of the trade-off study leading to the selection of an optimal plate scale for the Near-IR channel of the Wide Field Camera 3 (hereafter WFC3). The pixel sizes being considered range between 0.080'' and 0.160'', although the latter is challenging from an optical design and packaging point of view. Within this interval, and with the expected instrument and detector performance, the point source sensitivity is relatively independent of the pixel size while the extended source sensitivity improves with larger pixels.When factoring in the resulting gain of field of view (hereafter FOV), this trade-off becomes a balancing act between discovery efficiency, defined as the FOV divided by the exposure time to achieve a given S/N on a given point source, and point spread function (hereafter PSF) quality. The latter is clearly very important when studying faint sources near bright sources, as, e.g., in the case of quasar host galaxies or crowded field photometry.

These considerations lead us to consider in detail the properties of the PSF for the WFC3 instrument. Our reference PSF is the one of NICMOS camera 2, since its pixel size of 0.0768’’ makes it suitable for comparison with WFC3. The PSF properties and the various parameters quantifying them are discussed in Sect. 2.

Even with an ideal PSF the photometry of HST would be affected by the nature of infrared detectors. In NICMOS Camera 3 the counts obtained from a given star can vary by about 25 per cent depending on where the star is centered within a pixel (Fruchter et al. 1999; see also Lauer 1999). This is due to a combination of undersampling and dead space between pixels. This large photometric error can, in principle, be corrected. Clearly any correction will be more accurate if the effect is reduced, e.g., by better sampling the PSF. In order to gain an understanding of this effect, we have attempted to model the pixel dead-space. Our model for the pixel response is described in Sect. 3. Once a PSF for the camera optics and a model for the pixel response are available we can begin simulating realistic WFC3 Near-IR images and carry out stellar photometry on them. The simulations are described in Sect. 4, and the photometry results are described in Sect. 5. Sect. 6 summarizes our results.

2. The PSF of HST instruments

An ideal PSF described by an Airy function can be thought of as a single parameter family described by the FWHM. Unfortunately, HST and its instruments are not ideal and various physical effects break the simplicity of this one-parameter description. The calculations discussed in the following have been done using the method of Schroeder (1987).

As our reference example we compare the FWHM and the diameter of the aperture enclosing 50 per cent of the energy (hereafter EE). For an Airy function these two quantities are essentially identical and their value, for a primary mirror 2.4 meters in diameter, is 0.097’’ and 0.099’’ at 1.1 μ, respectively, and 0.141’’ and 0.144’’ at 1.6 μ.

The central obscuration of the primary of HST has a diameter of 0.792 meters and has the effect of both slightly sharpening the PSF FWHM and increasing the diameter of 50 per cent EE, i.e. it sharpens the core but transfers light to the PSF wings. The FWHM and the 50 per cent encircled energy diameter are now, respectively, 0.092’’ and 0.112’’ at 1.1 μ and, respectively, 0.133’’ and 0.163’’ at 1.6 μ.

However, an infrared instrument requires a cold stop to mask out thermal emission from the mirror supports and the hole in the primary. Using as a guide the cold stop of NICMOS camera 2, one has a reduction of the effective telescope diameter to 2.29 meters and an increase in size of the central obscuration to 0.828 meters. These affect the PSF by both increasing slightly its FWHM and transfering still more energy outside the PSF core. The FWHM and 50 per cent EE diameter are now, respectively, 0.095’’ and 0.121’’ at 1.1

μ and 0.138'' and 0.176'' at 1.6 μ. These values for FWHM and EE are still better than what is achieved in practice since one also has to account for the further PSF degradation caused by the secondary mirror supports and their masks in the cold stop, mainly due to a sizeable fraction of energy in the diffraction spikes. Another non-ideal effect to be included is the convolution of the monochromatic PSF over a given filter passband. Following "Tiny Tim" (Krist 1997) the PSF with a perfectly aligned cold stop has FWHM and 50 per cent EE diameter of, respectively, 0.090'' and 0.148'' in F110W and 0.135'' and 0.204'' in F160W. Unfortunately, either by construction or due to the stretching of the NICMOS dewar, the cold stop in NICMOS Camera 2 was misaligned, causing a further degradation of the PSF which, before pixelization, has FWHM and 50 per cent EE diameter of, respectively, 0.093'' and 0.180'' in F110W and 0.138'' and 0.230'' in F160W.

Our results are summarized in Table 1 and Figure 1. Note that while the FWHM of the PSF core remains very close to the value for the an ideal Airy function, the diameter of 50 per cent EE increases by 60 to 80 per cent. Figure 1 shows, for both F110W and F160W, the FWHM (filled symbols) and the diameters of 50, 65, 80, and 90 per cent encircled energies (EE, open symbols) for the cases discussed above. The Airy function values are given as triangles, values for an ideal HST with central obscuration as squares, those for an ideal NICMOS Camera 2 with cold stop as stars. The values for a non-pixelized Camera 2 PSF are given as circles.

Figure 1: FWHM (filled symbol) and encircled energy diameters (EE, open symbols) for F110W and F160W. See Text for a description of the various models.

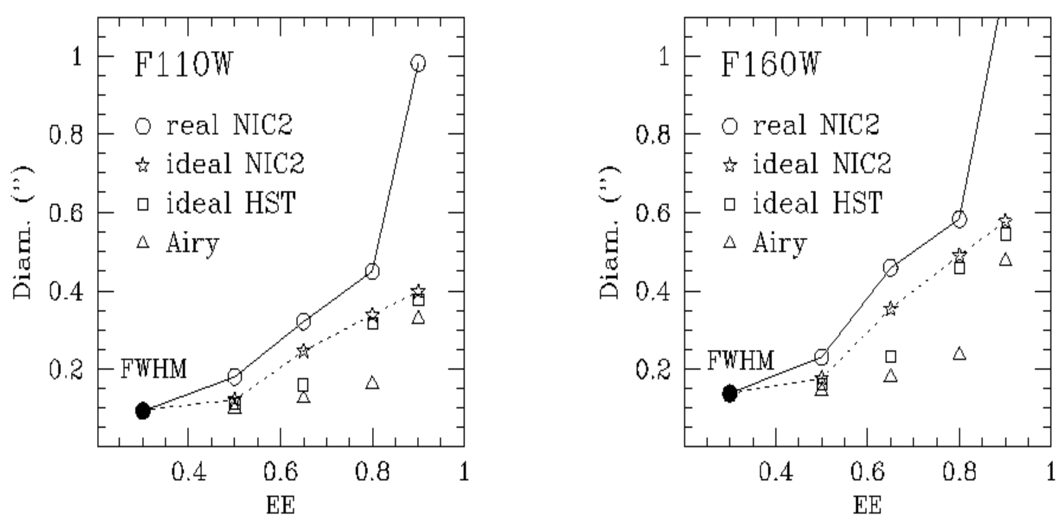

It is clear from the difference between the ideal and real NIC2 camera that it would be possible to improve the sensitivity of the infrared channel by improving the PSF, with particular regard to a reduction of the energy in the diffraction spikes.This would have a major impact on contrast and, consequently, on crowded field photometry. **Thus, we recommend that the possibility, cost, and benefits of apodizing the cold stop are studied.**

Table 1. Summary of the various effects on the PSF size (as discussed in the text)

PSF type	**FWHM (‘’)**	**50 % EE diameter (‘’)**
Airy-1.1μ	0.097	0.099
With Obscuration-1.1μ	0.092	0.112
Ideal NIC 2 Cold Stop-1.1μ	0.095	0.121
Aligned NIC2 -1.1μ	0.090	0.148
Real NIC2 -1.1μ	0.093	0.180
Airy-1.6μ	0.141	0.144
With Obscuration-1.6μ	0.133	0.163
Ideal NIC 2 Cold Stop-1.6μ	0.138	0.176
Aligned NIC2 -1.6μ	0.135	0.204
Real NIC2 -1.6μ	0.138	0.230

3. Non-uniform pixel sensitivity

We have considered the NIC3 camera with the F110W and F160W filters. This is the case discussed by Lauer (1999). Fruchter et al. (1999) have also carried out direct measurements on the Hubble Deep Field South (HDFS) data and found similar results to Lauer on the photometry in F160W but a smaller effect on F110W. The measurements are summarized in Figure 2 where we show, with different symbols, the data on four different bright stars in the HDFS NICMOS field. Each star is visible in 60 to 100 different dithered images. We find a clear correlation between the measured magnitudes within a 12 pixel aperture (in diameter) and the centroid position within a pixel. Results for different stars are similar. The measured effect is of about 25 per cent in both F110W and F160W with an rms scatter of 0.04 and 0.06 mag, respectively. This implies that the observed magnitudes of a bright stars in NIC3 can be corrected to within 0.04 mag in F160W with a single exposure. A much better correction is achievable if several dithered exposures are available. The distribution of magnitude shifts for F110W is non symmetrical with respect to the pixel center (as found also by Lauer 1999). If the symmetry center was used to determine the distance we would find a somewhat steeper slope and an rms scatter reduced to 0.045 mag for F110W.

On the basis of either an ideal or a NICMOS PSF, we have explored a simple physical model to account for the observed photometric error. In this model the effect is attributed to the presence of a dead space between pixels. Given an array with pixel-to-pixel separation d_pix, our model assumes that the geometrical pixel area d_pix $\times$ d_pix is larger than the effective active surface d_e $\times$ d_e where a pixel has non zero quantum efficiency. The dead space fractional linear size is d = 1- d_e/d_pix. In other words, each pixel can be regarded as a square of size d_e surrounded by a dead frame d/2 thick. The pixel response is assumed constant within the active area and zero outside. In this model any wavelength dependence of the effect would be purely a consequence of the PSF EE distribution.

Figure 2: Dependence of photometry on pixel position for NICMOS Camera 3

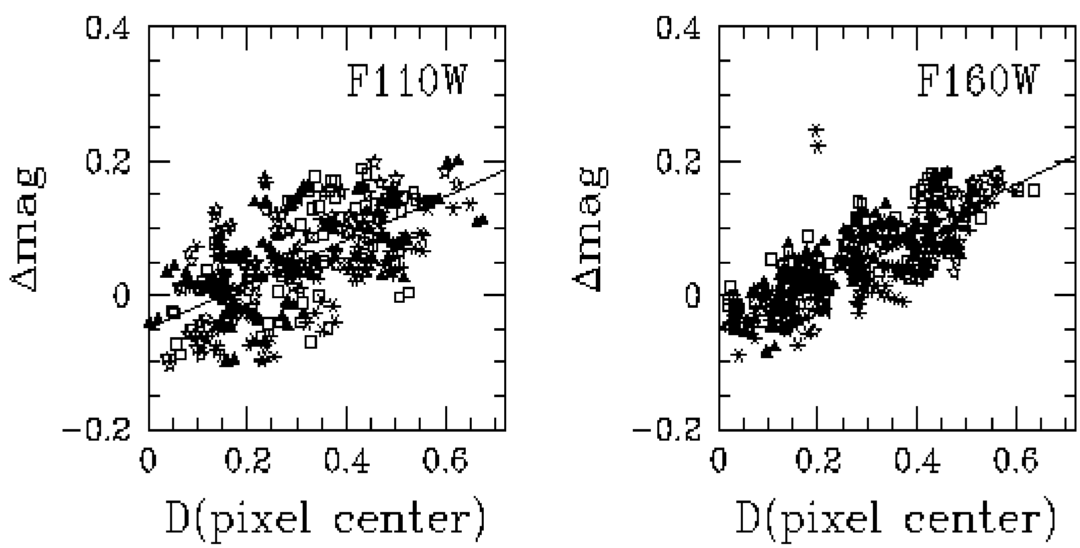

We have written an IDL program that takes the NICMOS PSF produced by “Tiny Tim” (Krist 1997) for both filters and rebins it to a scale corresponding to 1/20th of a NIC3 pixel. Then the PSF is projected 100 times on a 12×12 pixel matrix. The result is a grid of 10×10 digitized PSF which we can use to evaluate the absolute and relative photometric variations vs the centroid position. By varying the dead space, d, we can obtain results in good agreement with the observed behaviour of NICMOS Camera 3 for a value of d = 0.20. However, such a value for the interchip gap is at variance with the peak QE of a NICMOS array which exceeds 64 per cent at 2.2 μ. Thus it appears that our model, while suitable to represent the observations, does not capture the physical effect. An alternative (more realistic) possibility, is that the effect is caused by the fact that photons have to travel an implanted read-out electrode which is smaller than the pixel. The limited carrier mobility at the NICMOS operating temperature causes some of the carriers to be lost. This effect would be larger for shorter wavelength photons since they are detected closer to the surface. Within this model, surface irregularities may also explain the observed asymmetry in F110W. If this is indeed the explanation we expect that WFC3 arrays will not suffer significantly from this effect since in this case the carrier mobility is much higher due to the higher operating temperature. A full description of these results and additional modelling will be reported elsewhere.

Based on these results and on the presently available information concerning the dead space in the new generation Hawaii arrays, in our simulations we have adopted either an “expected“ d = 0.08 or a “pessimistic” d=0.20 as the relevant description of the dead space linear size for WFC3.

4. Simulated images

We simulated crowded globular cluster fields using the oversampled NIC2 PSF using the following procedure:

1. NIC2 PSFs were generated by “TinyTim” assuming perfect focus and oversampling the PSFs by a factor of 3. PSFs were made for both the F110W and F160W filters using filter throughput tables provided with TinyTim. The diameter of the PSF generated was 10".
2. The IRAF task "starlist" in the "artdata" package was used to generate a globular cluster star distribution. A list of 10,000 stars was generated using a "hubble" spatial density function and a "salpeter" luminosity function. The simulated stars span a range of 17 magnitudes.
3. The simulated image is generated using the task "mkobjects". The object list generated by "starlist" provides the cluster distribution and the TinyTim NIC2 PSF is used as the star PSF. The "mkobjects" task scales the NIC2 PSF by the simulated star magnitude provided by "starlist".

The final noiseless images sampled on a 0.0256’’ pixel scale are then processed using a program written in Fortran that produces the final images. This program carries out the following steps:

1. Resamples the input image to the desired pixel scale by taking into account the non-uniform response within a pixel;
2. Carries out dithering by simulating several pointings for each image. Typically a 2 by 2 matrix is used when the pixel is 0.1’’ and a 3 by 3 matrix is used for 0.15’’ since they allow us to produce a final drizzled image with 0.050’’ pixels;

3. Adds a gaussian read-out noise and a poissonian photon noise to the images. The simulated exposure time is kept constant so that the images drizzled 2 by 2 have longer simulated exposure time than those drizzled 3 by 3;
4. Reconstructs the final drizzled image with 0.050'' pixels using interlancing (a special case of the Fruchter-Hook drizzling algorithm applicable for exact offsets -see Figure 3).The final FWHM achieved with interlacing was 0.12'' with a 0.10'' pixel size and 0.15'' with a 0.15'' pixel size.

Figure 3: .F110W simulated image of a globular cluster with 0.1''/pixel.

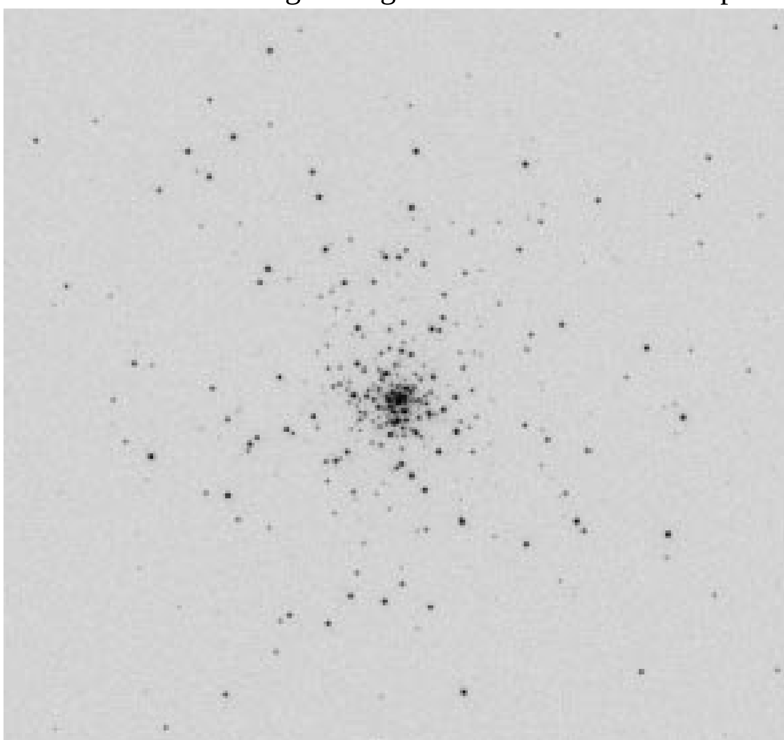

In this ISR we will concentrate on two F110W simulations:

1. **Version 1** : uses the actual NICMOS 2 PSF and an interpixel gap of d=0.08. The relative magnitude of the simulated stars is such that for the simulated ~15,000 seconds exposures there is a useful range of about 4 magnitudes. We believe that these are the most realistic simulations in terms of instrument parameters.
2. **Version 2**: uses a NICMOS 2 PSF with aligned cold stop and an interpixel gap of d=0.20. The relative magnitude of the simulated stars is such that for the simulated ~15,000 seconds exposures there is a useful range of about 10 magnitudes. Both the sharper, undersampled, PSF and the bigger gap affect negatively the photometric accuracy and thus these simulations represent a worst case scenario.

In the future, we are planning to repeat the simulations using an apodized PSF, rather than the actual NICMOS Camera 2 PSF, in order to explore the potential gains resulting from apodization. The simulated images have been made accessible to Science Oversight Committee to allow them to carry out additional measurements using different techniques.

5. Photometry

PSF-fitting photometry was carried out on the final simulated images using the DAOPHOT package created by P. Stetson and available in the IRAF "digiphot" package. We obtained accurate photometry for about 360 stars for the Version 1 images (see Figure 4) and 1350 stars for the Version 2 images (see Figure 5). Most stars were lost from the original 10,000 star sample because they were too faint to be detected above the read noise and poissonian photon noise introduced in the simulation. For the stars present in both the 0.1''/pixel and the 0.15''/pixel image the photometric errors were very similar: 0.13 and 0.14 mag, respectively, for Version 1 and 0.17 and 0.19 mag, respectively, for Version 2. Thus, **the larger pixel size does not significantly affect the photometric accuracy even for very crowded fields**.

Figure 4: Accuracy of simulated photometry on Version 1 reconstructed images (see text)

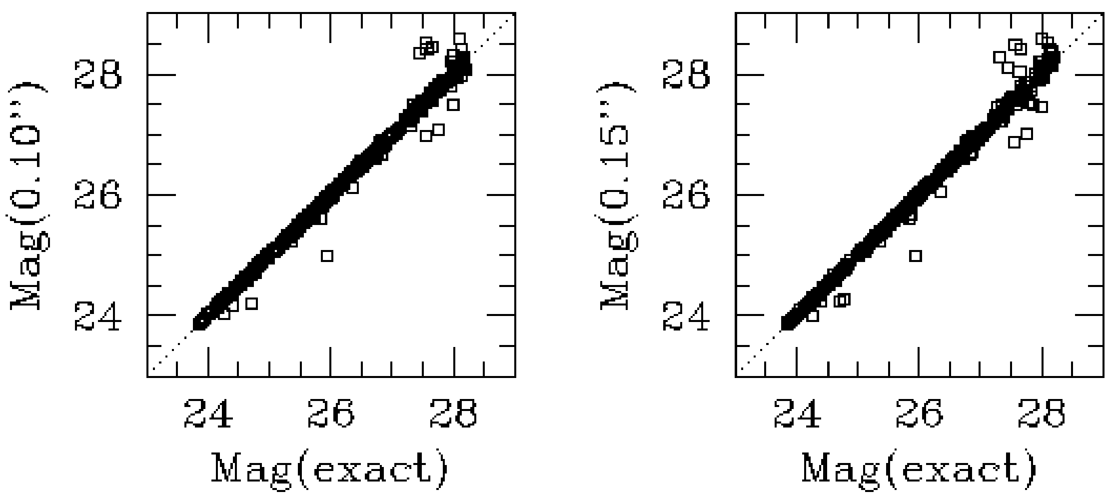

Figure 5: Accuracy of simulated photometry on Version 2 reconstructed images (see text)

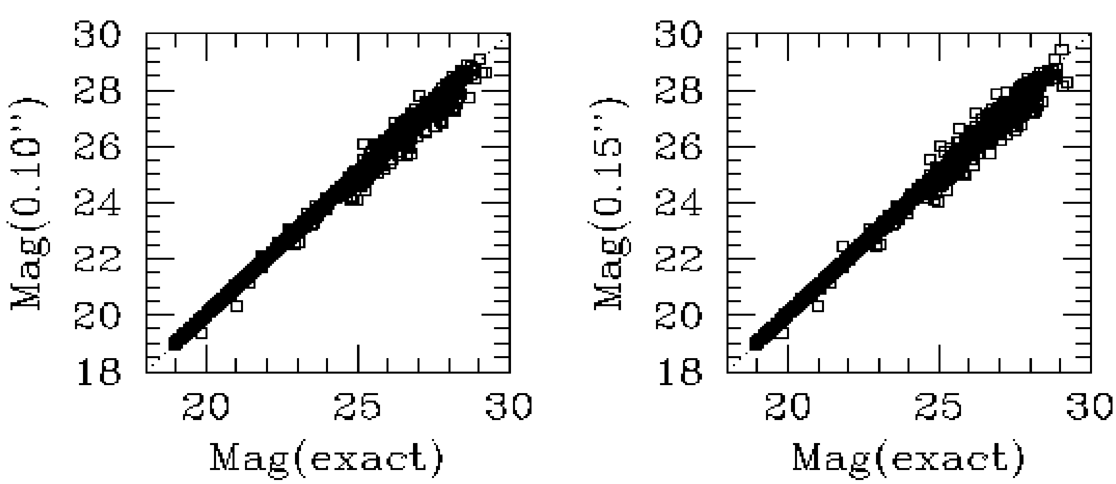

We have also investigated the effect of crowding on the completeness of our photometry. Our results are summarized in Figures 6 and 7 respectively for the Version 1 and Version 2 simulations. In the figures, the solid lines represent the input cumulative luminosity function, the dark grey (or red) squares the 0.1''/pixel photometry and the light grey (or cyan) circles the 0.15''/pixel photometry. The left panels are for the innermost one third of the stars (ie for a radius less than 3.75'' from the cluster center) and the right panels for all the stars. Particularly for the Version 2 simulation spurious detections of PSF structures are affecting the faint counts.

Figure 6: Cumulative counts for the Version 1 simulation (see text).

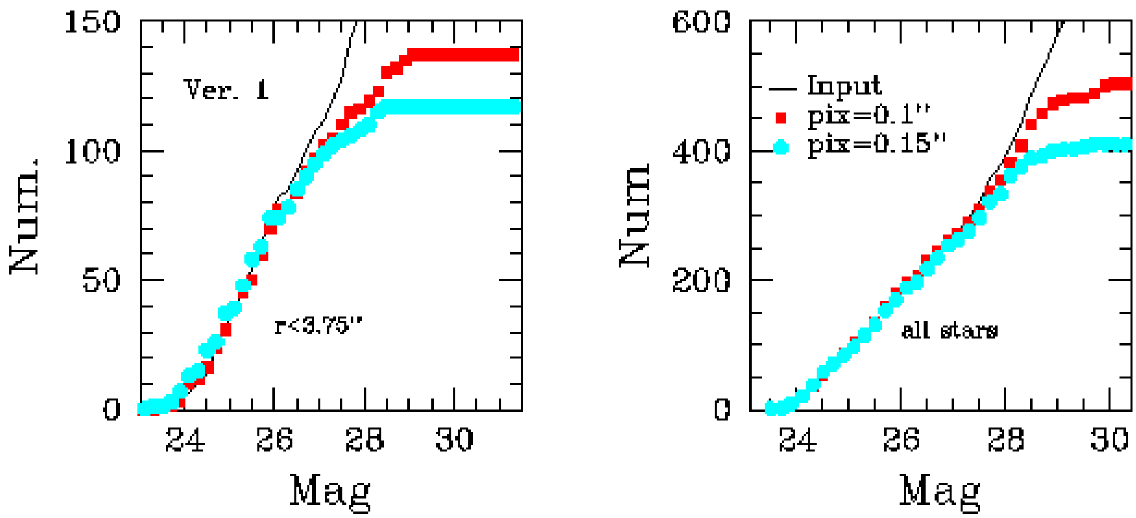

Figure 7: Cumulative counts for the Version 2 simulation (see text).

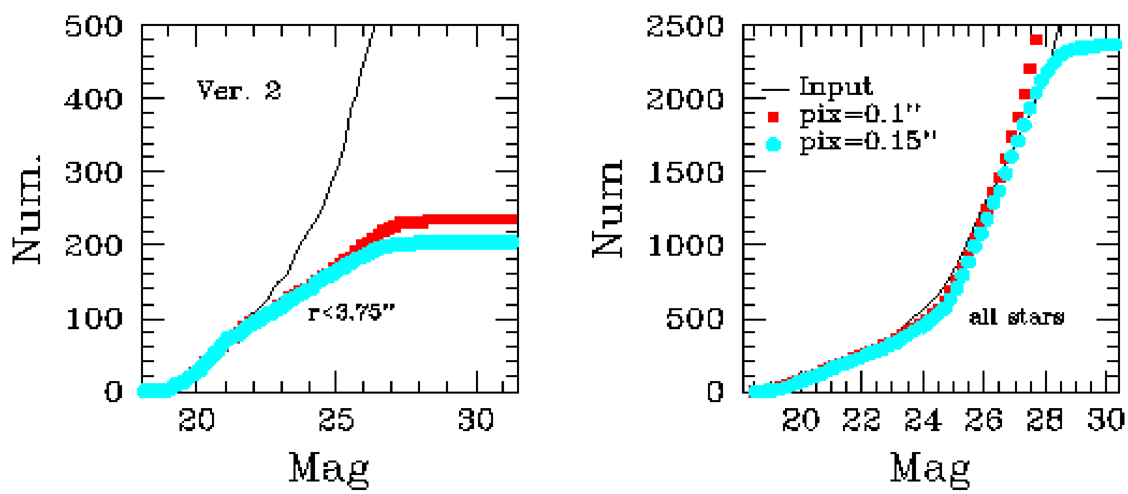

We find that the larger pixel size implies a loss in depth for the 90 per cent completeness level mostly due to crowding. The effect at the 80 per cent completeness level is instead rather modest. Our results are summarized in Table 2. An important comment regarding our completeness results is that whenever the difference between the 0.1''/pixel and the 0.15''/pixel results are significant, they are **both** diverging very strongly from the input luminosity function (see Figures 6 and 7). Once more the potential effect of a PSF with better encircled energy and less energy in the diffraction spikes could overwhelm any difference due to the pixel size. The image with the larger pixel size appears to be, at least in terms of completeness, less deep by about 0.3 to 1 mag. This difference is partly due to crowding and partly due to the image being intrinsically shallower by about 0.3 mag. This latter effect is understood in terms of the broader reconstructed PSF and a slightly shorter total exposure time (by 16.7 per cent) to account for the extra overhead of obtaining nine rather than four dithered positions.

Table 2. Completeness levels for the two simulations (see text)

	Version 1 (mag)		**Version 2 (mag)**	
	90 %	**80 %**	**90 %**	**80 %**
field center - 0.1''/pixel	27.2	27.7	22.1	22.8
field center - 0.15''/pixel	26.7	27.5	21.3	22.7
all stars - 0.1''/pixel	28.5	29.1	23.3	24.3
all stars - 0.15''/pixel	27.7	28.5	22.2	24.0

6. Conclusions

The conclusions of our study are the following:

1. For a constant exposure time the additional drizzling positions required by larger pixels and the broader resulting PSF can lead to a slight loss in depth. A reconstructed 0.15'' image appears to be less deep by about 0.3 magnitudes compared to a 0.1'' image;
2. The effective resolution achieved with drizzle was 0.12'' with a 0.10'' pixel size and 0.15'' with a 0.15'' pixel size;
3. Even with 0.3 magnitudes lost with the larger pixel size camera the increase in discovery efficiency for the 0.15''/pixel options remains of about 45 per cent;
4. Significant improvements in crowded field photometry could be obtained by improving the PSF quality.

7. Acknowledgements

We thank Brad Whitmore, Carey Lisse, and John Krist for useful suggestions, and Andy Fruchter for discussions on the performance of the drizzle algorithm.

8. References

Fruchter, A., and the HDFS NICMOS Team,1999, in preparation

Krist, J., 1997, Tiny Tim V.4.4 (see also http://scivax.stsci.edu/~KRIST/tinytim.html)

Lauer, T. D., 1999, submitted to PASP

Schroeder, D. J., 1987, *Astronomical Optics*, Academic Press (San Diego)